DATA ANALYSIS OF GRAVITATIONAL WAVE SIGNALS FROM COALESCING BINARIES

R. Balasubramanian[1]

Inter-University Center for Astronomy & Astrophysics
Ganeshkind
Pune

Abstract

In this lecture I shall be dealing with the techniques of Data analysis which will be used to extract the gravitational wave signal from the noisy output of the gravitational wave detector. The inspiral of binary systems consisting of compact objects such as black-holes and neutron stars can be well modelled. The knowledge of the signal waveform enables us to design detection strategies which are optimised to detect the 'chirp' signal. The basic idea here is to correlate the incoming data with the waveforms that we expect to observe.

[1]rbs@iucaa.ernet.in

Chandrasekhar is one of the most unusual examples of a scientist who has been able to inject his personal style into his work

— A. LIGHTMAN

He has an incomparable style. Good English style is a lost art in physics, but he has it and this wonderful feeling for the essential, and a feeling for beauty.

— V. WEISSKOPF

It's a rewarding aesthetic experience to listen to Chandra's lectures and study the development of theoretical structures at his hands. The pleasure I get is the same as I get when I go to an art gallery and admire paintings.

— LYMAN SPITZER

1 Introduction

Gravitational waves can be thought of as ripples in the curvature of spacetime which travel outward from the source carrying energy and momentum to the observer. These waves can be observed by measuring the proper distances between objects which are held fixed at constant coordinate positions in the observers reference frame.

The linear approximation to Einstein's equation yields the wave equation for the metric perturbation h_{ik} and thus gravitational waves are tensorial in nature. The magnitude of the the perturbation h_{ik} at the observer location can be written in terms of the derivatives of the quadrupole moment tensor

$$h_{ik}(t) = \frac{2G}{rc^4}\ddot{I}_{ik}(t - r/c). \tag{1}$$

This result is valid in the so called quadrupole or the 'Newtonian' approximation. An order of magnitude formula for h_{ik} can be given as

$$h \approx \frac{GE^{\text{kin}}_{\text{non-sph.}}}{c^4 r} \tag{2}$$

Gravitational waves carry a huge amount of energy. For a burst source in our galaxy such as a supernova for which the magnitude of $h_{ik} \approx 10^{-20}$ the flux on Earth would be around 30 Watts.m^{-2}! But the weak interaction of these waves with matter due to the smallness of G makes them hard to detect.

1.1 Sources and their strengths

A variety of sources are expected to be observed by the Earth based detectors which are currently being constructed. These are:

Binary Coalescences
: These are the most promising of all sources. Coalescences can be observed at cosmological distances. The typical magnitude for a NS/NS binary is about $h \approx 10^{-23}$ at a distance of 1000 Mpc. With the planned interferrometric detectors [1, 2] we would be observing the last few minutes before coalescence.

Supernovae
: The strength of these sources depends upon the degree of asymmetry during collapse. These will typically have a magnitude of $h \approx 10^{-18}, 10^{-19}$ for supernovae in our galaxy and will last for a few milliseconds.

Pulsars
: These are continuous wave sources with a typical magnitude of $h \approx 10^{-26}$ at a distance of 10 kpc.

Stochastic background
: Quantitative estimates of the cosmological stochastic background is highly model dependent. Pulsar timing observations have already provided tight constraints in fixing an upper bound on the magnitude. It might be possible to further constrain the strength of this background using the gravitational wave detectors.

1.2 The laser interferometer

When two masses are suspended a distance l apart then the change in the proper distance between them due to a gravitational wave of amplitude h is $\approx hl$. Two types of detectors are currently employed:

- Resonant bar detectors and

- Laser interferometers.

The bar detectors are essentially metallic cylinders (other geometries are being investigated) of large mass. These detectors are sensitive in a narrow frequency region around their natural resonant frequencies.

The laser interferometer illustrated in figure 1, converts path length changes to phase difference between laser light emerging from the two arms.

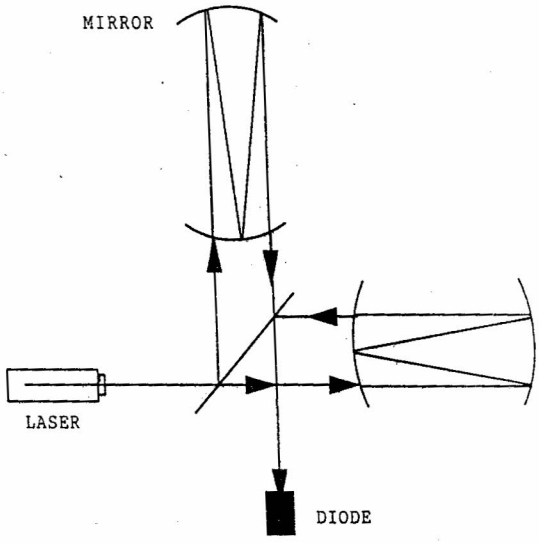

Figure 1: Schematic diagram of the laser interferometer

Such interferometers are being constructed by various groups around the world such as the American LIGO [1], the French-Italian VIRGO [2] and the German-English GEO. The LIGO will comprise of two four kilometre armlength detectors and one two kilometre armlength detector. The VIRGO will consist of a single three kilometre detector. whereas the GEO will have an armlength of 600 meters. A space based interferometric detector is also being planed and the launch is scheduled to take place in the year 2017. The interferometer as opposed to the resonant mass detector takes advantage of the quadrupolar nature of gravitational waves. The fluctuations in the proper distances between the mirrors can be estimated by measuring the shift of the fringe pattern at the photo diode. The laser interferometer is essentially a broadband device, which means that it is sensitive in a wide band of frequencies, though it can be made to operate at the narrowband mode by the use of dual recycling techniques. Ground based detectors will be typically able to measure gravitational waves at frequencies between $1 - 2000$Hz and hence we need to have very long light paths. This can partly be achieved by storing the laser power within a Fabry Perot cavity for a longer period of time. The laser interferometers have the advantage of being scalable, which means that the armlengths can be increased as and when it is feasible.

The performance of the detector will be limited by the various sources of noise. The four main sources of noise are

1. Seismic,
2. Thermal,
3. Photon shot,
4. Quantum noise

The lower cutoff of the detector is fixed by the seismic noise. This cutoff is between $1 - 10$Hz. There is a very steep falloff of this noise beyond the lower cutoff. Observation of gravitational

waves at frequencies lower than the seismic cut off will have to be done by space based detectors. The thermal noise is important at intermediate frequencies. As the apparatus will be maintained at room temperature the natural vibrations of the various normal modes of the mirrors and the suspension wires will be substantial. The thermal noise can be reduced by a careful selection of the material used for the construction of the mirrors. Also the effect of the thermal noise can be minimised by increasing the mass of the mirrors. Photon shot noise is important at large frequencies and is caused by the uncertainty in the number of photons at the photodiode. By increasing the power of the laser the effect of this noise can be reduced. The ultimate sensitivity of the detector will be decided by the quantum noise which is relatively less important as compared to the other kinds of noise.

To a large extent the noise in the detector will be Gaussian and hence the power spectrum of the noise describes it completely. The power spectrum $S_h(f)$ is defined by the relation

$$\overline{\tilde{n}(f)\tilde{n}^*(f')} = S_h(f)\delta(f - f'), \tag{3}$$

where $n(f)$ is the Fourier transform of the noise process $n(t)$. The power spectrum is a measure of the noise power per unit frequency and hence its square root measures the equivalent gravitational wave amplitude $h_{\rm eff}(f)$ which has been plotted in figure 2.

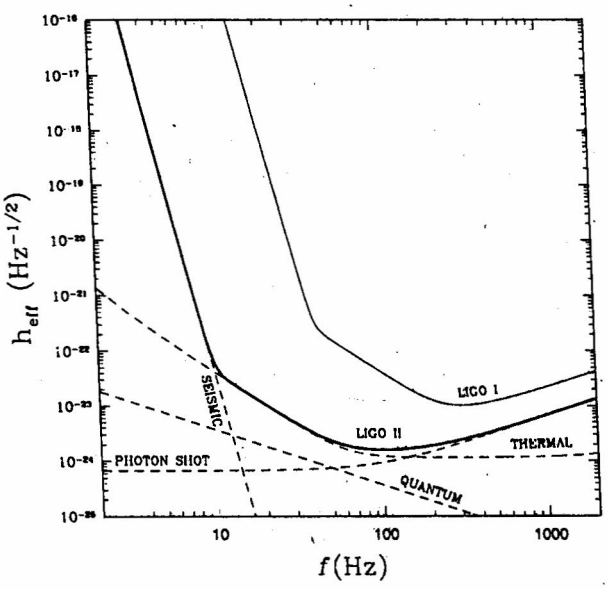

Figure 2: Noise spectrum of the LIGO interferometer

Figure 3 compares the sensitivity of the detector with the strength of the sources. For a signal of amplitude h and a average frequency f_c there is an enhancement of the signal by a factor $\sqrt{n}$ where n is the number of cycles in the neighbourhood of the frequency f_c. This has to be compared with the quantity $h_{\rm rms}$ which is the average strength of the noise over a single cycle of frequency f. For the case of burst sources lasting for a very short period the strength of the burst is to be compared with the quantity $h_{SB} = 11 h_{\rm rms}$.

2 Coalescing binaries

Coalescing binaries are promising sources of gravitational waves. The earth based interferometric detectors are ideally suited for measuring such gravitational waves. The key points are summarised

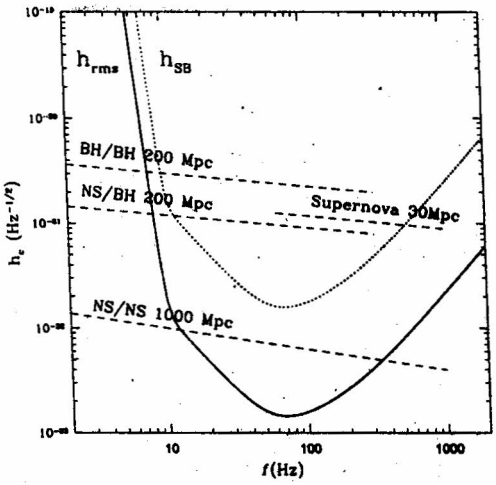

Figure 3: Comparison of the source strengths with the noise

below:

- Systems are well understood and modelled. This means that the waveform can be written down as a function of time and the parameters of the binary system such as the masses of the stars, their spins *etc.*
- The signal lasts for about 15 minutes in the bandwidth of the detector and we can integrate over this interval to enhance the signal to noise ratios.
- The event rates for such coalescences based on binary pulsar statistics have been carried out to a fair degree of reliability. The likely event rates are:
  - $\approx$ 3 NS/NS events per year upto 200Mpc,
  - $\approx$ 100 NS/NS events per year upto 1Gpc.

  These rates have also been extrapolated to BH/BH and BH/NS binaries. With the advanced detector we may be able to observe binaries at cosmological distances 1Gpc.
- The gravitational wave signal carries information of the masses, the spin angular momenta of the two components, the orientation of the binary, its direction, the eccentricity and its distance.
- The parameter information from a collection of such binaries can help determine the cosmologically relevant quantities:
  - the Hubble constant
  - the deceleration parameter
  - the cosmological constant
- Actual coalescence waveforms of BS/BS binaries will yield information about spacetime geometry in the extreme non-linear regime.
- Coalescence of NS/NS binaries will produce waveforms which are sensitive to the equation of state of nuclear matter.
- In the case of BH/NS binaries the tidal disruption of the neutron star can be studied.

2.1 Modelling the chirp waveform

The typical 'chirp' waveform is illustrated in figure 4. Both the amplitude and the frequency increase with time. As the two body problem has not been solved in general relativity post-Newtonian and post-Minkowskian schemes are followed to evaluate the waveform. It turns out that the phase evolution of the waveform is sensitive to the order to which the expansion has been carried out and this plays a major role in the detection strategy. For the purpose of my talk I shall restrict myself to a simplified model of the chirp waveform which is called the restricted post-Newtonian waveform. Here the higher harmonics of the waveform are neglected. Consequently,

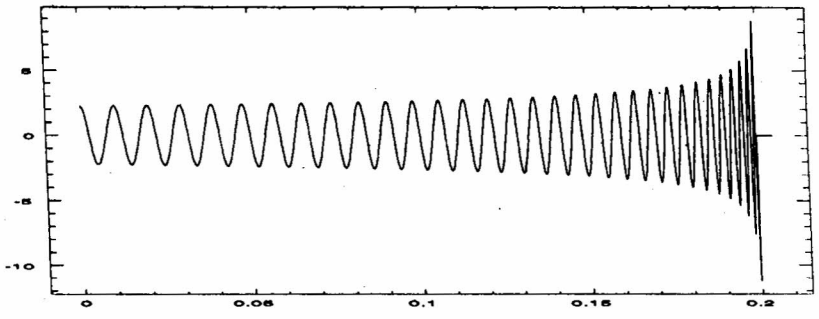

Figure 4: A typical chirp waveform

the restricted post-Newtonian waveforms only contain the dominant frequency equal to twice the orbital frequency of the binary computed up to the relevant order. In the restricted post-Newtonian approximation the gravitational waves from a binary system of stars, modeled as point masses orbiting about each other in a circular orbit, induce a strain $h(t)$ at the detector given by

$$h(t) = A(\pi f(t))^{2/3} \cos[\varphi(t)], \tag{4}$$

where $f(t)$ is the instantaneous gravitational wave frequency, the constant A involves the distance to the binary, its reduced and total mass, and the antenna pattern of the detector, and the phase of the waveform $\varphi(t)$ contains several pieces corresponding to different post-Newtonian contributions which can be schematically written as

$$\varphi(t) = \varphi_0(t) + \varphi_1(t) + \varphi_{1.5}(t) + \ldots. \tag{5}$$

Here $\varphi_0(t)$ is the dominant Newtonian part of the phase and φ_n represents the nth order post-Newtonian correction to it. To further simplify matters we give the formulae only upto the first post-Newtonian order:

$$t - t_a = \tau_0 \left(1 - \left(\frac{f}{f_a}\right)^{-8/3}\right) + \tau_1 \left(1 - \left(\frac{f}{f_a}\right)^{-1}\right)$$

$$\varphi(t) = 2\pi \int_{t_a}^{t} f(t')dt'$$

$$\varphi(t) = \frac{16\pi f_a \tau_0}{5} \left(1 - \left(\frac{f}{f_a}\right)^{-5/3}\right) + 4\pi f_a \tau_1 \left(1 - \left(\frac{f}{f_a}\right)^{-1}\right) + \Phi$$

$$\tau_0 = \frac{5}{256} M^{-1/3} \mu^{-1} (\pi f_a)^{-8/3}$$

$$\tau_1 = \frac{5}{192\mu (\pi f_a)^2} \left(\frac{743}{336} + \frac{11\mu}{4M}\right)$$

The quantities τ_0 and τ_1 have the physical significance of representing the Newtonian and post-Newtonian contribution to the time-of-coalescence starting from some fiducial time t_a. Thus in this approximation the time for coalescence is $\tau_0 + \tau_1$. Such a parameterization turns out to be very useful for signal analysis.

3 Detection of the chirp signal

The output of the detector is in general a superposition of a signal and noise. We now discuss how the signal can be extracted from the noisy output of the detector. We first discuss the concept of matched filtering and then develop a geometrical theory of signal analysis. Subsequently we will compare the results of the simulations of the detection process carried out with the theoretically expected results.

3.1 Matched filtering

In order to process the data from the detector the output $g(t)$ of the detector is passed through a linear time-invariant filter. The output of such a detector can be written as

$$c(\tau) = \int_{-\infty}^{\infty} g(t)q(t+\tau)dt = \int_{-\infty}^{\infty} \tilde{g}(f)\tilde{q}(f)e^{2\pi i f\tau}df$$

where $q(t)$ is the impulse response of the detector.

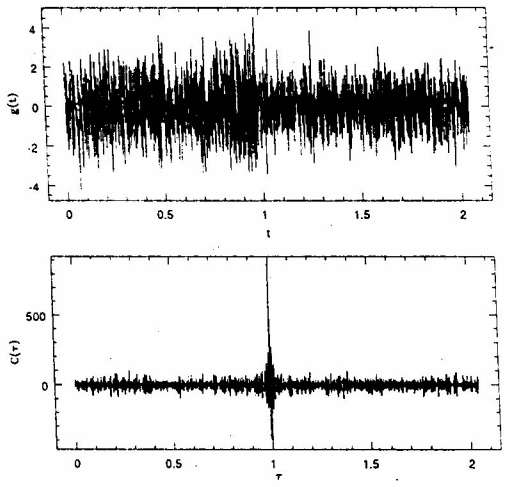

Figure 5: The graph at the top is a typical detector output data train. The noise being large it is difficult to infer the presence of the signal even though it is present. The graph in the bottom is the output of the filter which is matched to the signal present in the data train.

The graph in the top in figure 5 depicts a typical detector output data train which contains a gravitational wave signal from the coalescing binary. It is obvious that the presence of the signal cannot be inferred by inspection. It is necessary to employ special processing to extract the signal from the noise. Such a process is termed as a filter in signal analysis and we shall restrict ourselves to linear transformations of the detector output. The theory of optimal filtering enables us to select an optimal filter suited to the task.

In figure 5, the bottom graph, shows the output of the filter through which the detector output has passed. The key idea here has been to concentrate the signal energy spread over a finite time duration to a small amount of time. The presence of the signal is easily seen above the noise.

3.2 A Geometric approach to Signal analysis

The output of a gravitational wave detector will comprise of data segments, each of duration T seconds, uniformly sampled with a sampling interval of Δ, giving the number of samples in a single data train to be $N = T/\Delta$. Each data train can be considered as a N-tuple $(x^0, x^1, \ldots, x^{N-1})$ x^k being the value of the output of the detector at time $k\Delta$. The set of all such N-tuples constitutes an N-dimensional vector space $\mathcal{V}$ where the addition of two vectors is accomplished by the addition of corresponding time samples. For later convenience we allow each sample to take complex values. A natural basis for this vector space is the *time basis* $\mathbf{e}_m^k = \delta_m^k$ where m and k are the vector and component indices respectively. Another basis which we shall use extensively is the Fourier basis which is related to the time basis by a unitary transformation $\hat{U}$:

$$\tilde{\mathbf{e}}_m = \hat{U}^{mn}\mathbf{e}_n = \frac{1}{\sqrt{N}}\sum_{n=0}^{N-1}\mathbf{e}_n \exp\left[\frac{2\pi imn}{N}\right], \tag{6}$$

$$\mathbf{e}_m = \hat{U}^{\dagger mn}\tilde{\mathbf{e}}_n = \frac{1}{\sqrt{N}}\sum_{n=0}^{N-1}\tilde{\mathbf{e}}_n \exp\left[-\frac{2\pi imn}{N}\right]. \tag{7}$$

All vectors in $\mathcal{V}$ are shown in boldface, and the Fourier basis vectors and components of vectors in the Fourier basis are highlighted with a 'tilde'.

A gravitational wave signal from a coalescing binary system can be characterised by a set of parameters $\boldsymbol{\lambda} = (\lambda^0, \lambda^1, \ldots, \lambda^{p-1})$ belonging to some open set of the p-dimensional real space R^p. The set of such signals $\mathbf{s}(t; \boldsymbol{\lambda})$ constitutes a p-dimensional manifold $\mathcal{S}$ which is embedded in the vector space $\mathcal{V}$. The parameters of the binary act as coordinates on the manifold. The basic problem of signal analysis is thus to determine whether the detector output vector $\mathbf{x}$ is the sum of a signal vector and a noise vector, $\mathbf{x} = \mathbf{s} + \mathbf{n}$, or just the noise vector, $\mathbf{x} = \mathbf{n}$, and furthermore to identify which particular signal vector, among all possible. One would also like to estimate the errors in such a measurement. These statements are pictorially represented in figure 6.

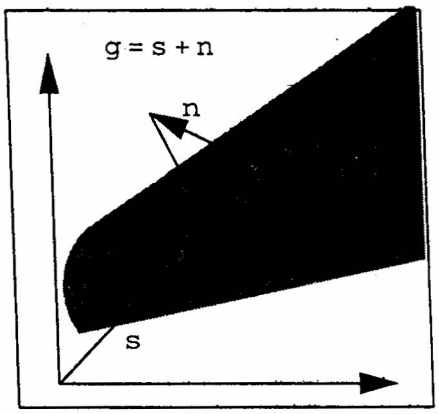

Figure 6: A pictorial representation of the signal manifold.

Essentially the detection process associates the detector output vector with a point on the manifold which is closest to it.

In the absence of the signal the output will contain only noise drawn from a stochastic process which can be described by a probability distribution on the vector space $\mathcal{V}$. The covariance matrix of the noise C^{jk} is defined as,

$$C^{jk} = \overline{n^j n^{*k}}, \tag{8}$$

where an * denotes complex conjugation and an overbar denotes an average over an ensemble. If the noise is assumed to be stationary and ergodic then there exists a noise correlation function

$K(t)$ such that $C_{jk} = K(|j-k|\Delta)$. In the Fourier basis it can be shown that the components of the noise vector are statistically independent [6] and the covariance matrix in the Fourier basis will contain only diagonal terms whose values will be strictly positive: $\tilde{C}_{jj} = \overline{\tilde{n}^j \tilde{n}^{*j}}$. This implies that the covariance matrix has strictly positive eigenvalues. The diagonal elements of this matrix $\tilde{C}_{jj}$ constitute the discrete representation of the power spectrum of the noise $S_n(f)$.

We now discuss how the concept of matched filtering can be used to induce a metric on the signal manifold. The technique of matched filtering involves correlating the detector output with a bank of filters each of which is tuned to detect the gravitational wave from a binary system with a particular set of parameters. The output of the filter, with an impulse response $\mathbf{q}$, is given in the discrete case as

$$c_{(m)} = \frac{1}{\sqrt{N}} \sum_{n=0}^{N-1} \tilde{x}^n \tilde{q}^{*n} \exp\left[-2\pi i m n/N\right]. \tag{9}$$

The SNR (ρ) at the output is defined to be the mean of $c_{(m)}$ divided by the square root of its variance:

$$\rho \equiv \frac{\overline{c_{(m)}}}{\left[\overline{\left(c_{(m)} - \overline{c_{(m)}}\right)^2}\right]^{1/2}}. \tag{10}$$

By maximising ρ we can obtain the expression for the optimal filter $\mathbf{q_{(m)}}$ matched to a particular signal $\mathbf{s}(t;\lambda^\mu)$ as

$$\tilde{q}^n_{(m)}(\lambda^\mu) = \frac{\tilde{s}^n(\lambda^\mu)\exp\left[2\pi i m n/N\right]}{\tilde{C}_{nn}}, \tag{11}$$

where ρ has been maximised at the m^{th} data point at the output and where $\mu = 1, 2, \ldots, p$ where p is the number of parameters of the signal. We now introduce a scalar product in $\mathcal{V}$. For any two vectors $\mathbf{x}$ and $\mathbf{y}$,

$$\langle \mathbf{x}, \mathbf{y} \rangle = \sum_{i,j=0}^{N-1} C^{-1}_{ij} x^i y^j = \sum_{n=0}^{N-1} \frac{\tilde{x}^n \tilde{y}^{*n}(\lambda^\mu)}{\tilde{C}_{nn}}. \tag{12}$$

In terms of this scalar product, the output of the optimal filter $\mathbf{q}$, matched to a signal $\mathbf{s}(\lambda^\mu)$, can be written as,

$$c_{(m)}(\lambda^\mu) = \frac{1}{\sqrt{N}} \langle \mathbf{x}, \mathbf{s} \rangle. \tag{13}$$

As $\tilde{C}_{kk}$ is strictly positive the scalar product defined is positive definite. The scalar product defined above on the vector space $\mathcal{V}$ can be used to define a norm on $\mathcal{V}$ which in turn can be used to induce a metric on the manifold. The norm of a vector $\mathbf{x}$ is defined as $\|\mathbf{x}\| = \langle \mathbf{x}, \mathbf{x} \rangle^{1/2}$. The norm for the optimal filter can be calculated to give $\rho = \langle \mathbf{s}, \mathbf{s} \rangle^{1/2}$. The norm of the noise vector will be a random variable $\langle \mathbf{n}, \mathbf{n} \rangle^{1/2}$ with a mean value of $\sqrt{N}$ as can be seen by writing the expression for the norm of the noise vector and subsequently taking an ensemble average.

The distance between two points infinitesimally separated on $\mathcal{S}$ can be expressed as a quadratic form in the differences in the values of the parameters at the two points:

$$g_{\mu\nu} d\lambda^\mu d\lambda^\nu \equiv \|\mathbf{s}(\lambda^\mu + d\lambda^\mu) - \mathbf{s}(\lambda^\mu)\|^2 = \left\| \frac{\partial \mathbf{s}}{\partial \lambda^\mu} d\lambda^\mu \right\|^2 \tag{14}$$

$$= \left\langle \frac{\partial \mathbf{s}}{\partial \lambda^\mu}, \frac{\partial \mathbf{s}}{\partial \lambda^\nu} \right\rangle d\lambda^\mu d\lambda^\nu. \tag{15}$$

The components of the metric in the coordinate basis are seen to be the scalar products of the coordinate basis vectors of the manifold.

Since the number of correlations we can perform on-line is finite, we cannot have a filter corresponding to every signal. A single filter though matched to a particular signal will also 'detect' signals in a small neighbourhood of that signal but with a slight loss in the SNR. The

drop in the correlation can be related to the metric distance on the manifold between the two infinitesimally separated signal vectors. In statistical theory the matrix $g_{\mu\nu}$ is called the Fisher information matrix.

In section 2.1 we have already introduced the waveform and the four parameters $\lambda^\mu = \{t_a, \Phi, \tau_0, \tau_1\}$. We now introduce an additional parameter for the amplitude and call it $\lambda^0 = \mathcal{A}$. The signal can now be written as $\tilde{s}(f;\lambda) = \mathcal{A}h(f; t_a, \Phi, \tau_0, \tau_1)$, where, $\lambda \equiv \{\mathcal{A}, t_a, \Phi, \tau_0, \tau_1\}$. Numerically the value of the parameter $\mathcal{A}$ will be the same as that of the SNR obtained for the matched filter provided $\mathbf{h}$ has unit norm. We can decompose the signal manifold into a manifold containing normalised chirp waveforms and a one-dimensional manifold corresponding to the parameter $\mathcal{A}$. The normalised chirp manifold can therefore be parameterized by $\{t_a, \Phi, \tau_0, \tau_1\}$. This parameterization is useful as the coordinate basis vector $\frac{\partial}{\partial \mathcal{A}}$ will be orthogonal to all the other basis vectors as will be seen below.

In order to compute the metric, and equivalently the Fisher information matrix, we use the continuum version of the scalar product as given in [11], except that we use the two sided power spectral density. This has the advantage of showing clearly the range of integration in the frequency space though we get the same result using the discrete version of the scalar product. Using the definition of the scalar product we get

$$g_{\mu\nu} = \int_{f_a}^{\infty} \frac{df}{S_n(f)} \frac{\partial \tilde{s}(f;\lambda)}{\partial \lambda^\mu} \frac{\partial \tilde{s}^*(f;\lambda)}{\partial \lambda^\nu} + \text{c.c.} \tag{16}$$

It turns out that the signal manifold associated with the chirp signal is flat and moreover the particular set of parameters that we have chosen turn out to constitute a cartesian coordinate system on the chirp manifold.

3.3 Choice of filters

It is obvious that as the number of signals is infinite one cannot correlate the output with every possible signal and we must choose a discrete set of templates which will do the job. The most obvious strategy would be to take a finite number of points on the signal manifold, evenly placed on the signal manifold. However it might be much more efficient not to restrict the set of templates to lie on the manifold. Such a strategy has been implemented in [15] and the results obtained are encouraging.

3.4 Estimation of parameters

We have seen that the detection process involves correlating the detector output with a host of templates. The most likely parameters of the binary are same as those of the template which obtains the maximum correlation with the detector output. We would like to compute the errors inherent in such a measurement. We define the error matrix

$$\epsilon^{\mu\nu} = \overline{\left(\lambda^\mu - \overline{\lambda}^\mu\right)\left(\lambda^\nu - \overline{\lambda}^\nu\right)}. \tag{17}$$

It can be shown [6] that there in a lower bound to the errors in such a measurement. This bound is called the Cramer-Rao bound and in the limit of high SNRs the errors converge to the Cramer-Rao bound. The Cramer-Rao bound is valid for unbiased maximum likelihood estimates, conditions which the matched filtering statistic satisfies. It turns out that the lower bound turns out to be nothing but the inverse of the Fisher information matrix or equivalently the inverse of the metric on the signal manifold. Thus,

$$\epsilon^{\mu\nu} \geq g^{-1}_{\mu\nu} = C^{\mu\nu}. \tag{18}$$

In order to test the validity of these bounds we carried out extensive numerical simulations. The simulations were carried out by adding numerous realizations of noise to a given signal and then filtering it through a bank of filters. The simulations were carried out were representative of the actual detection process. The assumptions made are listed below:

1. The initial LIGO power spectrum was used mainly because of computational reasons.

2. We considered BH-NS and BH-BH binaries as their coalescence time is less as compared to low mass binaries. This leads to lesser computational requirements.

3. Only the restricted first post-Newtonian waveform was used. We ignored the spins in the waveform.

4. The inspiral of the binary is abruptly cut of by the plunge phase which occurs when the two stars are approximately at a distance of $6m$ from each other. As the exact onset of the plunge is uncertain we carried out the simulations with the plunge effect both included and excluded.

5. The range of SNRs which we worked with, were between 10 and 20.

3.5 Results of simulations

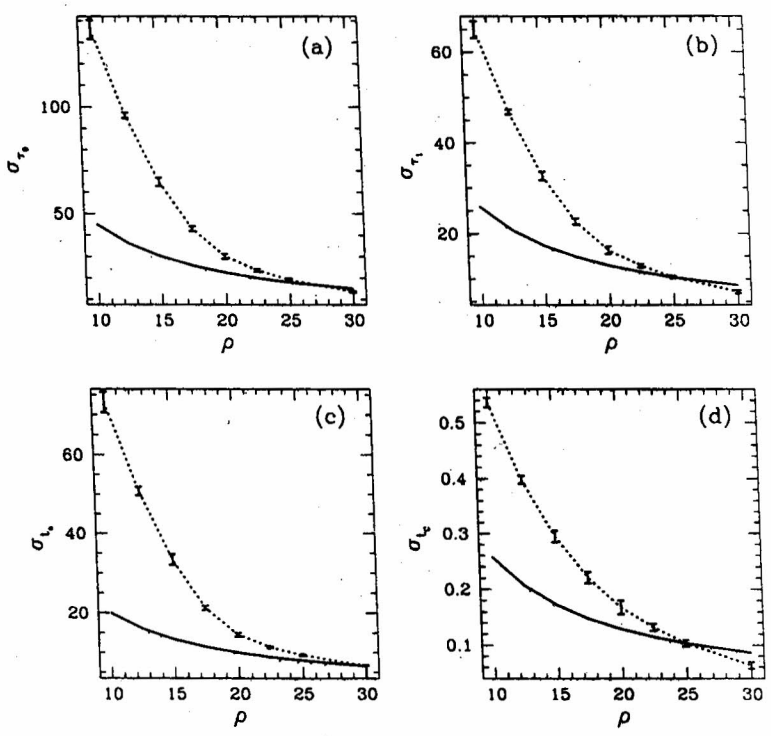

Figure 7: Dependence of the errors in the estimation of parameters of the post-Newtonian waveform *i.e.* $\{\sigma_{\tau_0}, \sigma_{\tau_1}, \sigma_{t_a}, \sigma_{t_C}\}$ as a function of SNR. The solid line represents the analytically computed errors whereas the dotted line represents the errors obtained through Monte Carlo simulations.

The results of the simulations are shown in figure 7. We compare the actual errors obtained with the covariance matrix. The results are shown for the parameters τ_0, τ_1, t_a and $t_C = \tau_0 + \tau_1 + t_a$. The parameter t_C is termed as the instant of coalescence and is very accurately determined.

There is a huge discrepancy in the errors obtained via simulations and the errors obtained by the covariance matrix at SNRs of about 10. Due to the intrinsic weakness of gravitational wave sources, we should not expect to see sources with SNRs higher that 10 very frequently. There is approximately a factor of three difference between the two. This implies that more careful

estimation of the errors would have to be carried out. At a SNR of about 30 the errors are in good agreement with the covariance matrix. It is to be noted that the experimental errors are less than the lower bound at high SNRs. This is partly due to numerical noise in the simulations and partly due to the fact that the covariance matrix itself is evaluated using a numerical integration routine. Moreover the accuracy can also be improved by increasing the sampling rate and hence improving the resolution in time.

4 Conclusion

We have discussed here issues in the data analysis of the gravitational wave signals from coalescing binary systems. Though a lot of work has been done in this area a lot of scope remains to improve the detection strategies to be employed. We enumerate below the directions which future work in this area can take.

1. More accurate waveforms are needed so as to improve the chances of detection.
2. To obtain more realistic bounds on the error matrix. As we have seen the Cramer Rao bound works only for very high signal to noise ratios.
3. Further use of differential geometry in choosing templates optimally.
4. Exploration of other data analysis techniques, such as:
   - Periodogram
   - Resampling algorithms
   - non-linear filtering
   - wavelets
5. Optimisation of coincident detections among detectors spread around the globe. This is termed as the network problem.

References

[1] A. Abramovici *et. al.*, Science **256** 325 (1992).

[2] C. Bradaschia *et. al.*, Nucl. Instrum. Methods Phys. Res., Sect A 518 (1990).

[3] B.F. Schutz, in *Gravitational Collapse and Relativity,* Edited by H. Sato and T. Nakamura, (World Scientific, Singapore, 1986), pp. 350-368.

[4] D. Marković, Phys. Rev. D **48**, 4738 (1993).

[5] K.S. Thorne, in *300 Years of Gravitation*, S.W. Hawking and W.Israel (eds.), (Cambridge Univ. Press, 1987).

[6] C.W. Helstrom, *Statistical Theory of Signal Detection,* 2nd. ed, (Pergamon Press, London, 1968).

[7] B.F. Schutz, in *The Detection of Gravitational Radiation,* edited by D. Blair (Cambridge, 1989) pp 406-427.

[8] B.S. Sathyaprakash and S.V. Dhurandhar, Phys. Rev. D **44**, 3819 (1991).

[9] S.V. Dhurandhar and B.S. Sathyaprakash, Phys. Rev. D **49**, 1707 (1994).

[10] C. Cutler and E. Flanagan, Phys.Rev. D **49**, 2658 (1994).

[11] L.S. Finn and D.F. Chernoff, Phys. Rev. D **47**, 2198 (1993).

[12] B.S. Sathyaprakash, Phys. Rev. D **50**, R7111 (1994).

[13] C. Cutler *et al*, Phys. Rev. Lett. **70**, 2984 (1993).

[14] S. V. Dhurandhar and B.F. Schutz, Phys. Rev. D **50**, 2390 (1994)

[15] R. Balasubramanian, S.V. Dhurandhar and B.S. Sathyaprakash, Phys. Rev. D **53**, 3033 (1996).

I have been able to *think* more about stars than I would have, because of the lack of 'paper and pencil.' Paper and pencil necessarily land one in the intricacies of the calculation! I have a number of ideas and I am getting almost impatient to get back to Cambridge to work them out.

— S. CHANDRASEKHAR